Mycorrhizal distributions impact global patterns of carbon and nutrient cycling

R. K. Braghiere[1,2†], J. B. Fisher[1,2], R. A. Fisher[3,4], M. Shi[1,2], B. S. Steidinger[5], B. N. Sulman[6], N. A. Soudzilovskaia[7], X. Yang[6], J. Liang[8,9], K. G. Peay[5], T. W. Crowther[10], R. P. Phillips[11]

[1] Jet Propulsion Laboratory, California Institute of Technology, 4800 Oak Grove Drive, Pasadena, CA, 91109 USA.

[2] Joint Institute for Regional Earth System Science and Engineering, University of California at Los Angeles, Los Angeles, CA, 90095 USA.

[3] Climate and Global Dynamics Division, National Center for Atmospheric Research, Boulder, CO, USA.

[4] Laboratoire Évolution & Diversité Biologique, CNRS:UMR 5174, Université Paul Sabatier, Toulouse, France.

[5] Department of Biology, Stanford University, Stanford, CA, USA.

[6] Environmental Sciences Division and Climate Change Science Institute, Oak Ridge National Laboratory, Oak Ridge, TN, USA.

[7] Environmental Biology Department, Institute of Environmental Sciences, Leiden University, Leiden, The Netherlands.

[8] Department of Forestry and Natural Resources, Purdue University, West Lafayette, IN, USA.

[9] Research Center of Forest Management Engineering of State Forestry and Grassland Administration, Beijing Forestry University, Beijing, China.

[10] Department of Environmental Systems Science, ETH Zürich, Zürich, Switzerland.

[11] Department of Biology, Indiana University, 1001 E Third St, Bloomington, IN 47403, USA.

Corresponding author: Dr. Renato K. Braghiere (renato.k.braghiere@jpl.nasa.gov)

† Current address: Jet Propulsion Laboratory, M/S 233-305F, 4800 Oak Grove Drive, Pasadena, CA, 91109 USA.

Supplementary Materials Document

Includes:

- Supplementary Information
- Supplementary Tables
- Supplementary Figures
- Supplementary References

Supplementary information

Land Surface model description: the Community Land Model version 5 (CLM5)

CLM5 is the land surface component of the Community Earth System Model 2 (CESM2; https://www.cesm.ucar.edu/models/cesm2/). CLM5 includes three important changes to the representation of plant carbon and nitrogen dynamics: i) the Leaf Utilization of Nitrogen for Assimilation (LUNA) module allows plants to adjust their partitioning of nitrogen among the maximum rate of carboxylation (V_{cmax}), the maximum rate of electron transport (J_{max}), and other leaf nitrogen components, to achieve co-limitation of photosynthesis under the prevailing time-averaged environmental drivers (CO_2, temperature, humidity, soil moisture, radiation, and day length) (Xu et al., 2012; Ali et al., 2016; Fisher et al., 2019); ii) the 'FlexCN' module allows plants to alter and optimize their stoichiometry, removing the down-regulation of gross primary productivity (GPP) that was used in CLM4 and CLM4.5 (Cheng et al., 2019; Ghimire et al., 2016). In the new allocation algorithm, the total nitrogen supply in each timestep is partitioned among tissues in proportion to their relative 'demand' terms. Additional details on how stoichiometry is optimized can be found in Lawrence et al. (2019) and Fisher et al. (2019); and finally, iii) the Fixation and Uptake of Nitrogen (FUN) module implements a 'carbon cost' for each source of plant nitrogen uptake (Fisher et al., 2010; Brzostek et al., 2014; Shi et al., 2016; Allen et al., 2020).

The carbon cost of nitrogen uptake from soil by mycorrhizal or non-mycorrhizal pathways, for each soil layer j, is controlled by two uptake parameters that pertain respectively to the relationship between soil nitrogen and nitrogen uptake, and between fine root carbon density and nitrogen uptake. For mycorrhizal or non-mycorrhizal nitrogen uptake, the cost functions are given as:

$$N_{cost,pathway,j} = \frac{k_{n,pathway}}{N_{smin,j}} + \frac{k_{c,pathway}}{c_{root,j}} \quad (1.0)$$

where $k_{n,\mathrm{pathway}}$ (kgC.m^{-2}) and $k_{\mathrm{c,pathway}}$ (kgC.m^{-2}) varies according to whether the pathway considered is referring to a non-mycorrhizal (direct), ECM, or AM uptake. $N_{smin,j}$ and $c_{root,j}$ are the soil nitrogen content (gN.m^{-3}) and fine root carbon density (gC.m^{-3}), respectively. Please refer to CLM5 technical note and related publications (Fisher et al., 2019; Lawrence et al., 2019; NCAR, 2019) for the complete set of equations.

Shi et al. (2016) classified the Plant Functional Types (PFTs) in CLM, based upon known associations between plant species and either arbuscular mycorrhizae (AM) or ectomycorrhizae (ECM) fungi described in the literature (Read, 1991; Allen et al., 1995; Phillips et al., 2013). While some PFTs are usually AM-dominated (e.g., grasslands), others are usually ECM-dominated (e.g., boreal forest). PFT symbiont fraction estimates are available as ratios of the AM-associated and ECM-associated plants of the CLM PFTs as a table in Shi et al. (2016). These numbers are usually binary, associating one PFT with a single type of mycorrhizae, e.g., 0% or 100%, except for broadleaf deciduous temperate trees, which associates 50% with AM and 50% with ECM.

Coupling mycorrhizae spatial distribution into CLM5

In CLM5, within each grid cell, the soil area available for vegetation is divided into patches that correspond to the area fraction of that PFT. For each PFT, a number of key parameters are defined, such as the target tissue C:N values, stomatal water use efficiency, maximum hydraulic conductivity and sensitivity to embolism (Kennedy et al., 2019), tissue allocation fractions (for leaves, fine roots, stem, and coarse roots), tissue turnover times, and the rate at which litter class (labile, lignin, cellulose) decays and returns nutrients to the soil after death. Four global maps of mycorrhizal association based on different assumptions and spatial resolutions were added into CLM5 to provide the percentage of ECM association (relative to

AM) data for CLM5: Map A (Shi et al., 2016); Map B (Sulman et al., 2019), Map C (Steidinger et al., 2019), and Map D (Soudzilovskaia et al., 2019) (**Fig. 1**).

Map B was derived from Sulman et al. (2019), who assembled empirical AM data points presenting species number of AM fungi obtained from the MAARJAM database (Öpik et al., 2010), and ECM data points presenting species number of ECM fungi obtained from Tedersoo et al. (2014). These data were used to define niche models which were used to develop spatial maps of the relative probability of AM and ECM fungal presence within areal units of 10 arcmin. These niche models were used to estimate ECM fraction by comparing the relative probability of AM and ECM presence:

$$\%ECM = 100*p(ECM)/(p(ECM) + p(AM)) \quad (2.0)$$

where p(ECM) and p(AM) are the probabilities of ECM or AM presence, respectively, from the niche model in each grid cell.

Map C was derived from Steidinger et al. (2019), who proposed a global map of the symbiotic status of forests, using a database of over 1 million forest inventory plots containing more than 28,000 tree species, and 70 global predictor layers: 19 climatic indices (relating to annual, monthly, and quarterly temperature and precipitation variables), 14 soil chemical indices (relating to soil nitrogen density, microbial nitrogen, C:N ratios and soil P fractions, pH and cation exchange capacity), 26 vegetative indices (relating to leaf area index, total stem density, enhanced vegetation index means and variances), and 5 topographic variables (relating to elevation and hillshade). Their maps provide quantitative estimates of the distribution of aboveground biomass fractions among AM, ECM, and N fixers plants within areal units of 0.5° and 1.0°.

Map D was proposed by Soudzilovskaia et al. (2019), who assembled a global database on plant mycorrhizal type associations that included 2,169 studies and 27,736 species-by-site records for 12,702 plant species and combined it with information about dominant plant species and their growth form across distinct combinations of Bailey's with 98 ecoregions (Bailey, 2014) and European Space Agency (ESA) land cover categories (ESA, 2017) with spatial resolution of 300 m. Their maps provide quantitative estimates of the distribution of aboveground biomass fractions among AM, ECM, and ericoid mycorrhiza (ERM) plants withins areal units of 10 arcmin.

The maps D and B are principally different from maps A and C. Consequently, conversions to unify the data for comparisons have to be applied. Map D shows fractions of biomass for all plants, not only trees, while the map B shows the likelihood of occurrence of ECM biomass in a grid cell based on a species distribution model fit to a genomic database. Sulman et al. (2019) produced a range from very low likelihood of ECM fungal DNA being present in observations to higher likelihood of ECM presence. In order to compare map B with other maps, the ECM map was first combined with the AM map and normalized, producing a spectrum that incorporates both mycorrhizal types.

A regridding process of the maps to CLM5 grid scales was applied by calculating an average value for ECM in percentage per PFT per gridcell based on the GLC2000 land cover data (Bartholomé & Belward, 2005) at a spatial resolution of 500 m following a look-up table (**Supplementary Table S1**). The average value of ECM percentage was assigned to one of the 16 particular natural vegetation PFTs in CLM5 per gridcell, assuming that AM and ECM trees do not differ in biomass. In this case, using basal area maps and biomass percentages map interchangeably is acceptable in tree-dominated areas. In other areas, it is assumed that although differences in the data products might exist, the nature of the measure is assumed to have little impact, as long as given in the format of a ratio of ECM over ECM plus AM present in the grid cells, due to the fact that CLM5 ingests the data as a ECM ratio per PFT.

Table S1. Look-up table between GLC Global Class and CLM PFTs.

CLM PFT	Classification	GLC Global Class
PFT 0	Bare soil (not vegetated)	(19)Bare Areas
PFT 1	Needleleaf evergreen temperate tree	(04)Tree Cover, needle-leaved, evergreen; (06)Tree Cover, mixed leaf type; (07)Tree Cover, regularly flooded, fresh water (& brackish); (08)Tree Cover, regularly flooded, saline water; (09)Mosaic; (10)Tree Cover, burnt; (17)Mosaic;

PFT 2	Needleleaf evergreen boreal tree	(04)Tree Cover, needle-leaved, evergreen; (06)Tree Cover, mixed leaf type; (07)Tree Cover, regularly flooded, fresh water (& brackish); (08)Tree Cover, regularly flooded, saline water; (09)Mosaic; (10)Tree Cover, burnt; (17)Mosaic;
PFT 3	Needleleaf deciduous boreal tree	(05)Tree Cover, needle-leaved, deciduous; (06)Tree Cover, mixed leaf type; (07)Tree Cover, regularly flooded, fresh water (& brackish); (08)Tree Cover, regularly flooded, saline water; (09)Mosaic; (10)Tree Cover, burnt; (17)Mosaic;
PFT 4	Broadleaf evergreen tropical tree	(01) Tree Cover, broadleaved, evergreen; (06)Tree Cover, mixed leaf type; (07)Tree Cover, regularly flooded, fresh water (& brackish); (08)Tree Cover, regularly flooded, saline water; (09)Mosaic; (10)Tree Cover, burnt; (17)Mosaic;
PFT 5	Broadleaf evergreen temperate tree	(01) Tree Cover, broadleaved, evergreen; (06)Tree Cover, mixed leaf type; (07)Tree Cover, regularly flooded, fresh water (& brackish); (08)Tree Cover, regularly flooded, saline water; (09)Mosaic; (10)Tree Cover, burnt; (17)Mosaic;
PFT 6	Broadleaf deciduous tropical tree	(02)Tree Cover, broadleaved, deciduous, closed; (06)Tree Cover, mixed leaf type; (07)Tree Cover, regularly flooded, fresh water (& brackish); (08)Tree Cover, regularly flooded, saline water; (09)Mosaic; (10)Tree Cover, burnt; (17)Mosaic;
PFT 7	Broadleaf deciduous temperate tree	(02)Tree Cover, broadleaved, deciduous, closed; (06)Tree Cover, mixed leaf type; (07)Tree Cover, regularly flooded, fresh water (& brackish); (08)Tree Cover, regularly flooded, saline water; (09)Mosaic; (10)Tree Cover, burnt; (17)Mosaic;
PFT 8	Broadleaf deciduous boreal tree	(02)Tree Cover, broadleaved, deciduous, closed; (06)Tree Cover, mixed leaf type; (07)Tree Cover, regularly flooded, fresh water (& brackish); (08)Tree Cover, regularly flooded, saline water; (09)Mosaic; (10)Tree Cover, burnt; (17)Mosaic;

PFT 9	Broadleaf evergreen shrub	(01) Tree Cover, broadleaved, evergreen; (06)Tree Cover, mixed leaf type; (09)Mosaic; (11)Shrub Cover, closed-open, evergreen; (13)Herbaceous Cover, closed-open; (14)Sparse Herbaceous or sparse Shrub Cover; (15)Regularly flooded Shrub and/or Herbaceous Cover; (17)Mosaic; (18)Mosaic
PFT 10	Broadleaf deciduous temperate shrub	(03)Tree Cover, broadleaved, deciduous, open; (06)Tree Cover, mixed leaf type; (09)Mosaic; (12)Shrub Cover, closed-open, deciduous; (13)Herbaceous Cover, closed-open; (14)Sparse Herbaceous or sparse Shrub Cover; (15)Regularly flooded Shrub and/or Herbaceous Cover; (17)Mosaic; (18)Mosaic
PFT 11	Broadleaf deciduous boreal shrub	(03)Tree Cover, broadleaved, deciduous, open; (06)Tree Cover, mixed leaf type; (09)Mosaic; (12)Shrub Cover, closed-open, deciduous; (13)Herbaceous Cover, closed-open; (14)Sparse Herbaceous or sparse Shrub Cover; (15)Regularly flooded Shrub and/or Herbaceous Cover; (17)Mosaic; (18)Mosaic
PFT 12	C3 arctic grass	(09)Mosaic; (13)Herbaceous Cover, closed-open; (14)Sparse Herbaceous or sparse Shrub Cover; (15)Regularly flooded Shrub and/or Herbaceous Cover; (17)Mosaic; (18)Mosaic
PFT 13	C3 nonarctic grass	(09)Mosaic; (13)Herbaceous Cover, closed-open; (14)Sparse Herbaceous or sparse Shrub Cover; (15)Regularly flooded Shrub and/or Herbaceous Cover; (17)Mosaic; (18)Mosaic
PFT 14	C4 grass	(09)Mosaic; (13)Herbaceous Cover, closed-open; (14)Sparse Herbaceous or sparse Shrub Cover; (15)Regularly flooded Shrub and/or Herbaceous Cover; (17)Mosaic; (18)Mosaic
PFT 15	Corn	(09)Mosaic; (16)Cultivated and managed areas; (17)Mosaic; (18)Mosaic

PFT 16	Wheat	(09)Mosaic; (16)Cultivated and managed areas; (17)Mosaic; (18)Mosaic
PFT 17	NaN	(20)Water Bodies (natural & artificial); (21)Snow and Ice (natural & artificial); (22)Artificial surfaces and associated areas; (23)No data

*****(09) Mosaic: Tree cover / Other natural vegetation; (17) Mosaic: Cropland / Tree Cover / Other natural vegetation; (18) Mosaic: Cropland / Shrub or Grass Cover.

Table S2. Average carbon cost values per unit nitrogen (gN.kgC^{-1}) from 2000 to 2010 for each different pathway and sum for all new maps and the default one in CLM5.

Pathway cost	**Reference**	**TRANSIENT – 2000 – 2010**				
(gN.kgC^{-1})	**Map A (CLM5)**	**Map B**	**Map C**	**Map D**	**Average (B,C,D)**	**Change (%)**
NMYC	1.15	1.15	1.21	1.04	1.13	1.4%
NFIX	104.00	103.80	105.20	107.60	105.53	-1.5%
NRETRANS	925.00	924.00	905.00	914.00	914.33	1.2%
NNONMYC	115.53	115.13	130.00	124.97	123.01	-6.5%
TOTALN	38.33	38.07	36.62	37.82	37.50	2.2%

Table S3. Average values from 2000 to 2010 of nitrogen uptake for each one of the different pathways and sum for the spatially distributed PFT based.

2000-2010

Pathway	**Reference**	**TRANSIENT – 2000 – 2010**		
(TgNyr-1)	**Map A (CLM5)**	**Map B**	**Map C**	**Map D**
NECM	10.7	10.8	14.8	7.5
NAM	9.9	9.8	8.7	11.8
NFIX	52.0	51.9	52.6	53.8

NRETRANS	92.5	92.4	90.5	91.4
NNONMYC	808.7	805.9	793.0	799.8
TOTALN	973.7	970.8	959.5	964.4

Table S4. Average values from 2000 to 2010 of carbon costs of nitrogen uptake for each one of the different pathways and sum for the spatially distributed PFT based. The values of CLM4-FUN from Shi et al. (2016) are shown as reference.

	1995-2004	***2000-2010***			
Pathway	**Reference**	**Reference**	**TRANSIENT - 2000 - 2010**		
(PgCyr-1)	**CLM4-FUN**	**Map A (CLM5)**	**Map B**	**Map C**	**Map D**
NPP_MYC	1.2	17.9	17.9	19.4	18.6
NPP_NFIX	0.4	0.5	0.5	0.5	0.5
NPP_NRETRANS	0.6	0.1	0.1	0.1	0.1
NPP_TOTAL N	2.4	25.4	25.5	26.2	25.5
NPP_NPASSIVE	0.0	0.0	0.0	0.0	0.0
NPP_NDIRECT	0.2	7.0	7.0	6.1	6.4

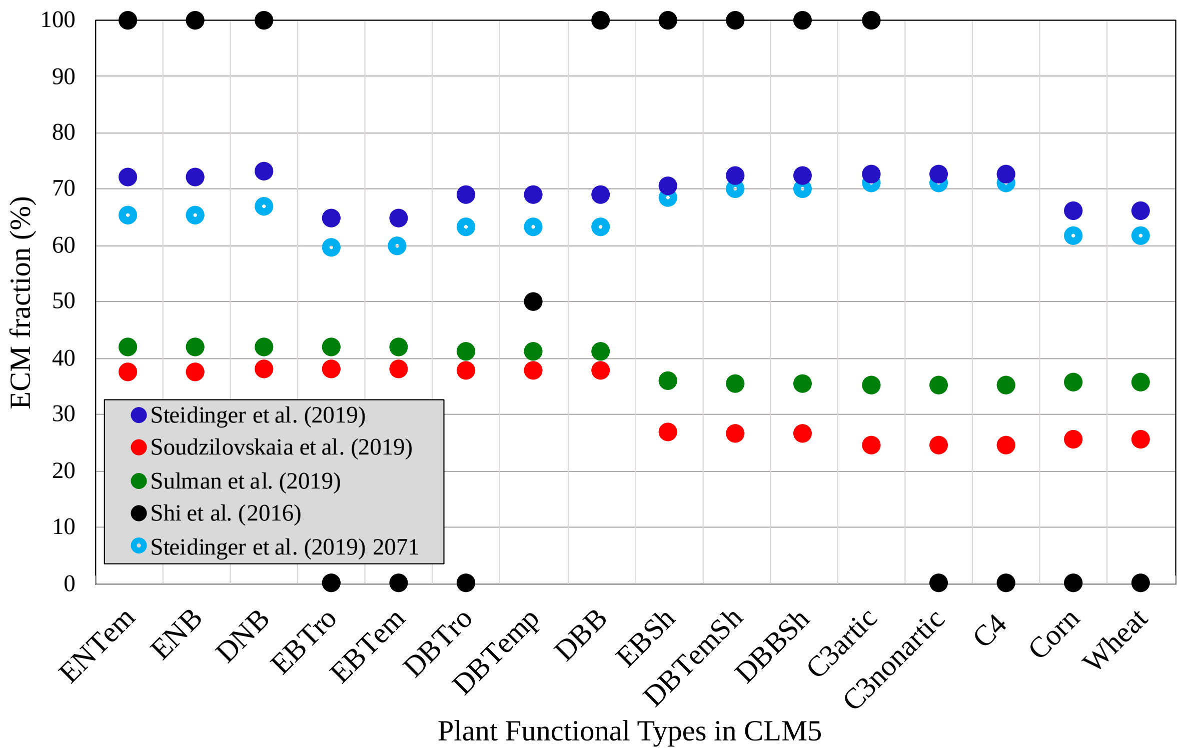

Figure S1. PFT global average of ECM fraction in percentage for ref. (Sulman et al., 2019); ref. (Steidinger et al., 2019) present and future (2071); ref. (Soudzilovskaia et al., 2019) and the base map in CLM5 as in ref. (Shi et al., 2016).

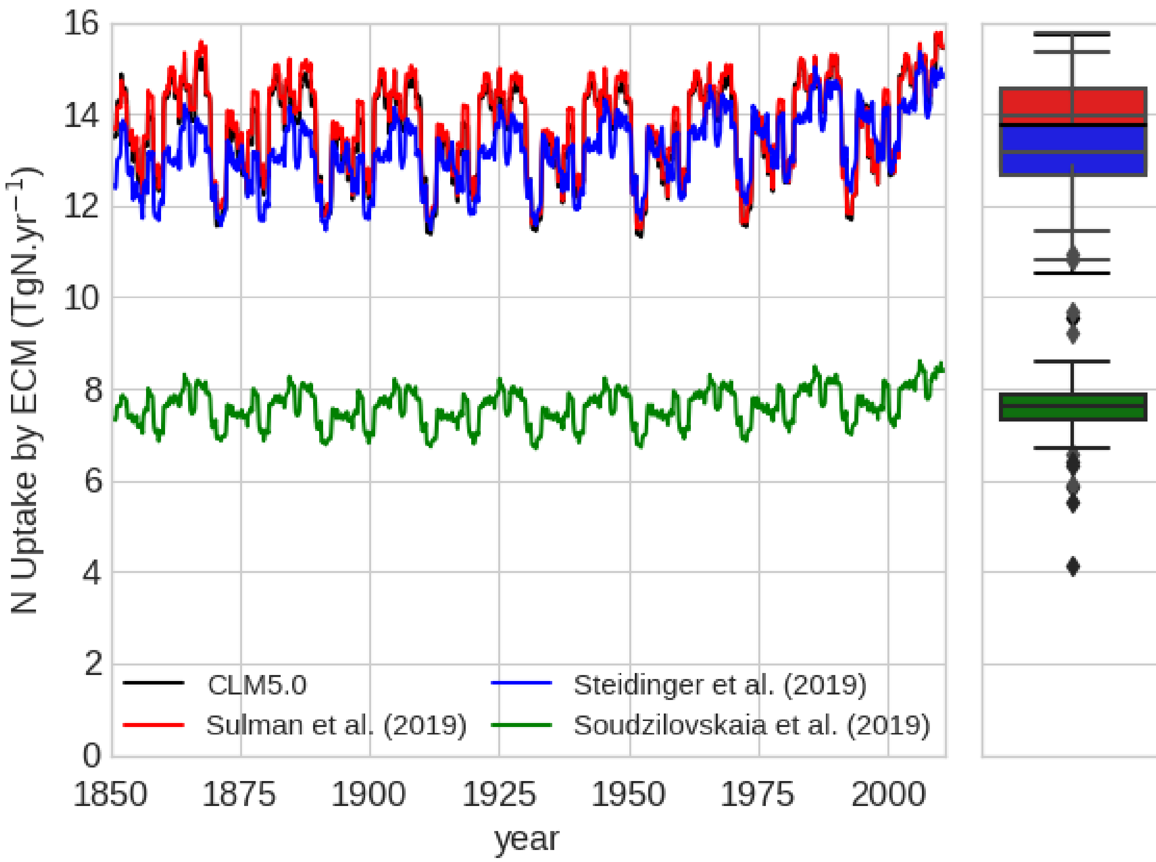

Figure S2. Nitrogen uptake through ectomycorrhizal association (NECM) in $TgNyr^{-1}$ for the transient run (1850-2010) for ref. (Sulman et al., 2019); ref. (Steidinger et al., 2019); and ref. (Soudzilovskaia et al., 2019) and the base map in CLM5 as in ref. (Shi et al., 2016) based on fixed PFT values.

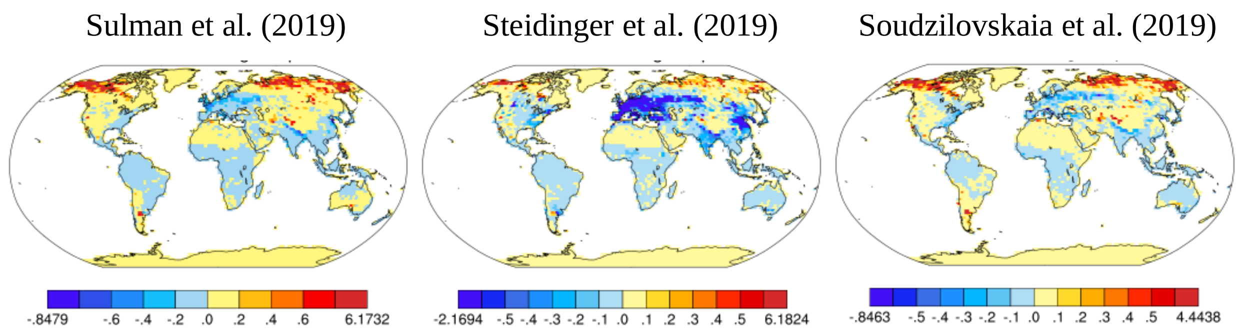

Figure S3. Revised global AM N uptake ($gNm^{-2}y^{-1}$) spatial distribution between **a.** Sulman et al. (2019); **b.** Steidinger et al. (2019); and **c.** Soudzilovskaia et al. (2019) and the base map in CLM5 as in Shi et al. (2016) based on PFT values per grid cell.

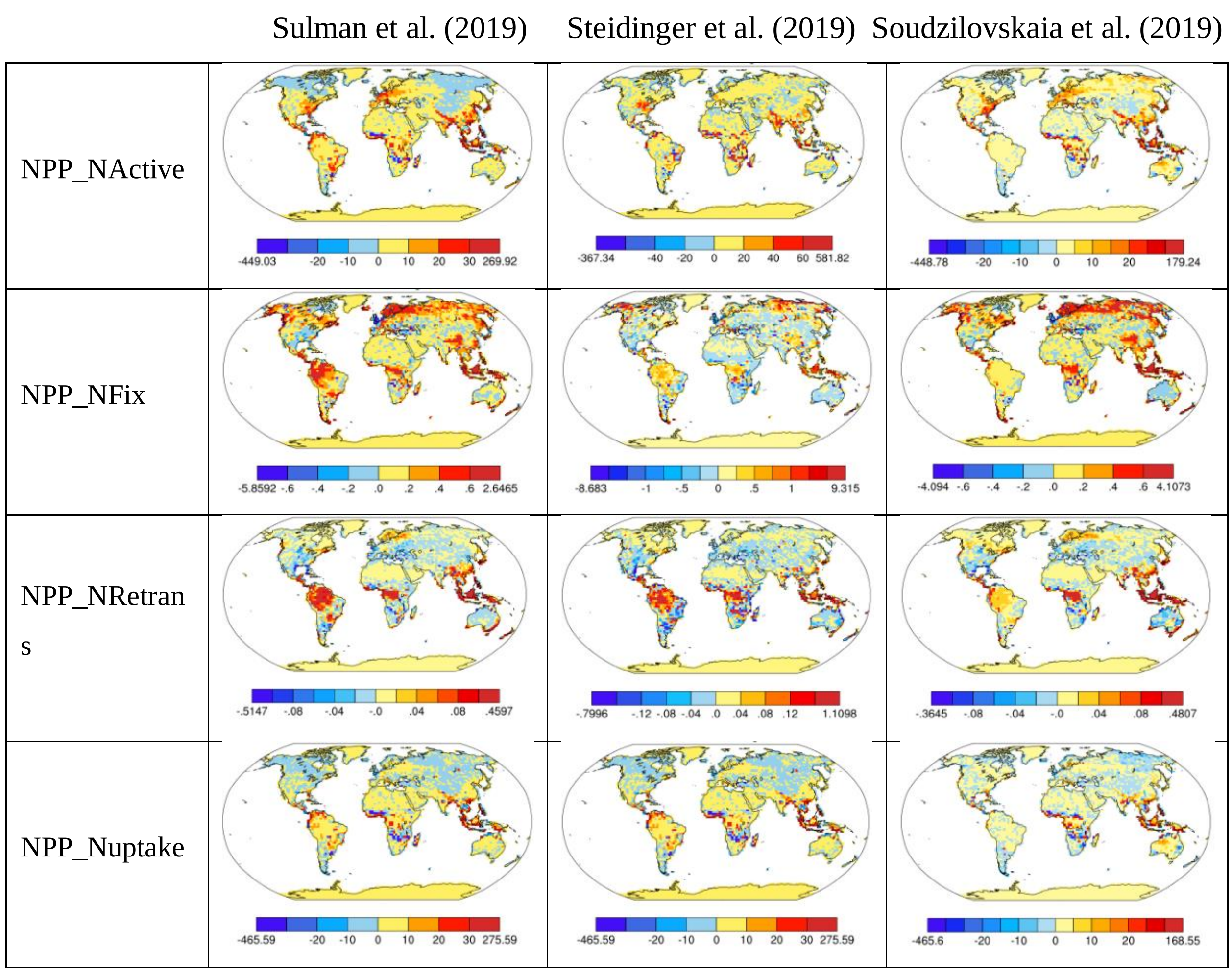

Figure S4. Revised carbon used for nitrogen uptake ($gCm^{-2}y^{-1}$) spatial distribution between a. Sulman et al. (2019); b. Steidinger et al. (2019); and c. Soudzilovskaia et al. (2019) and the base map in CLM as in Shi et al. (2016) based on PFT values per gridbox for different pathways: Mycorrhizal (NPP_NActive), Symbiotic BNF (NPP_NFix), retranslocated N (NPP_NRetrans), and total (NPP_Nuptake).

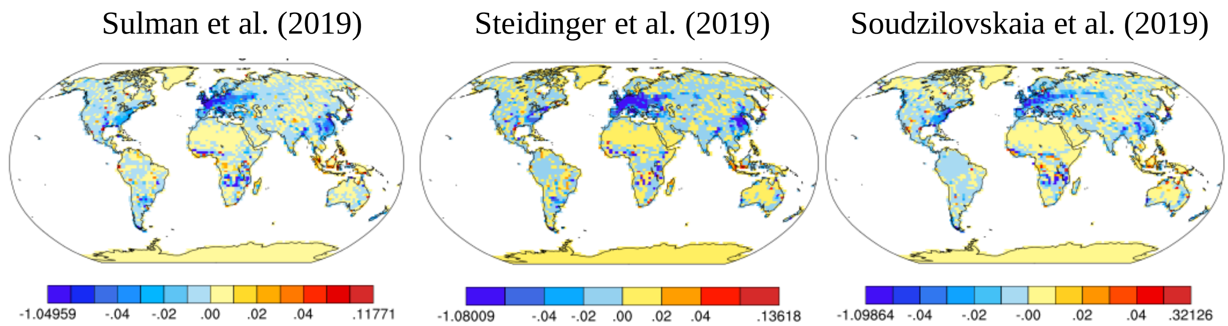

Figure S5. Revised Autotrophic Respiration ($gCm^{-2}y^{-1}$) spatial distribution between **a.** Sulman et al. (2019); **b.** Steidinger et al. (2019); and **c.** Soudzilovskaia et al. (2019) and the base map in CLM as in Shi et al. (2016) based on fixed PFT values (**above**) and based on PFT values per gridbox (**below**).

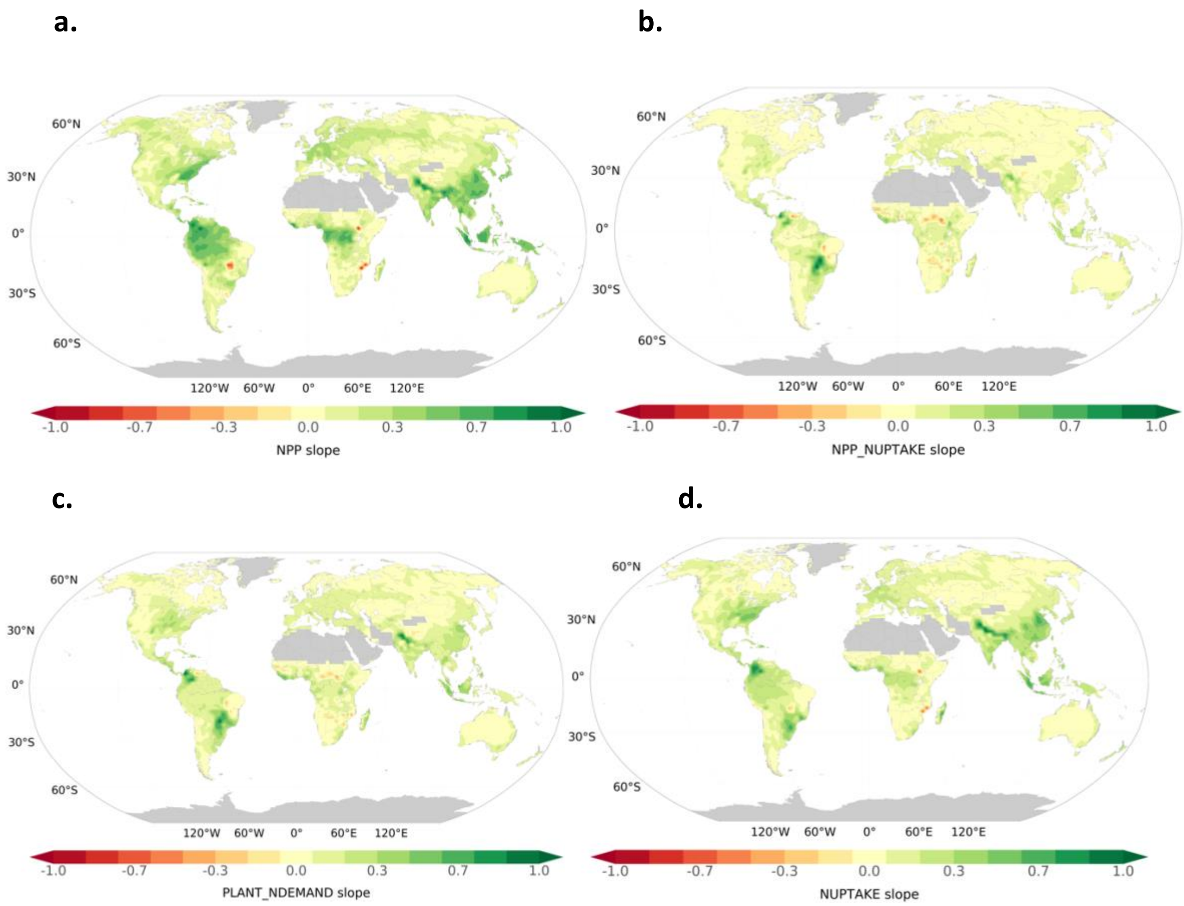

Figure S6. Normalized linear regression slope of **a.** NPP, **b.** NPP_NUPTAKE, **c.** PLANT_NDEMAND, and **d.** NUPTAKE with time.

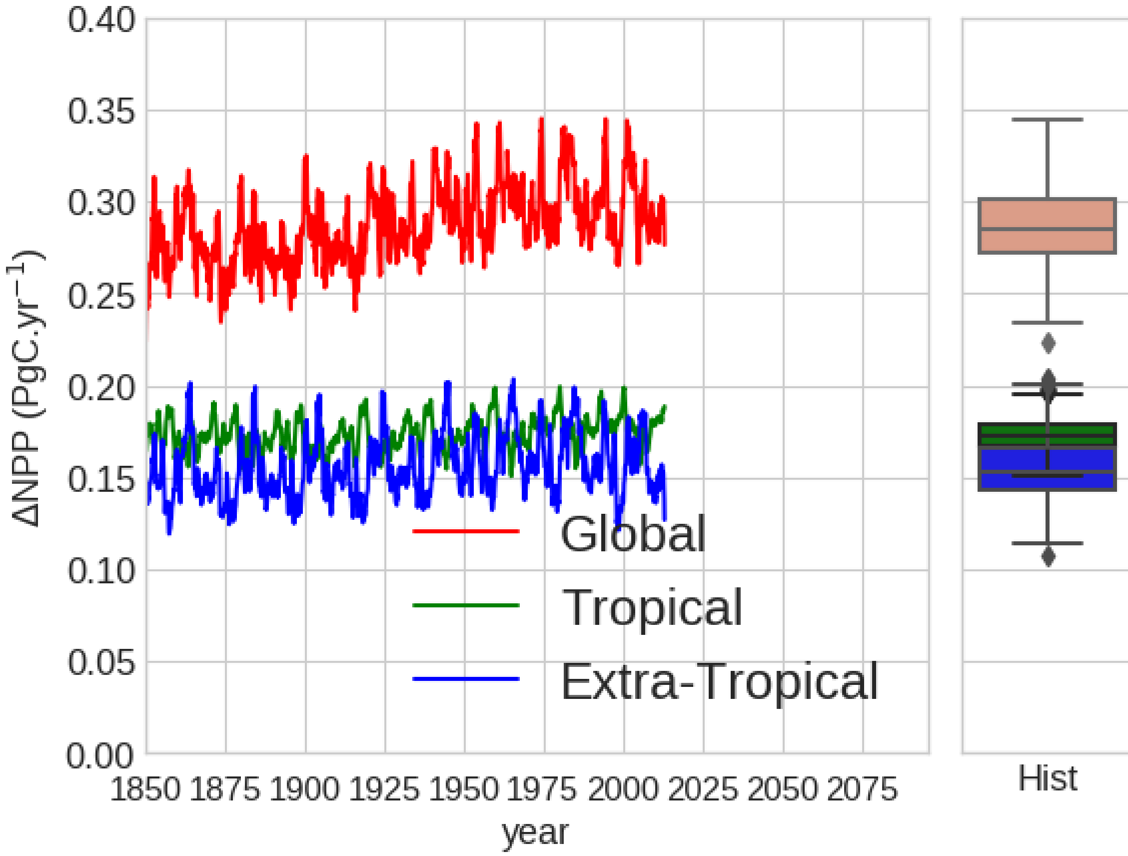

Figure S7. Global average maximum ΔNPP (PgC.yr^{-1}) for the transient historical runs from 1850 to 2010 with CLM5 for all different ECM maps.

References

Ali, A. A., Xu, C., Rogers, A., Fisher, R. A., Wullschleger, S. D., Massoud, E. C., et al. (2016). A global scale mechanistic model of photosynthetic capacity (LUNA V1.0). *Geoscientific Model Development*, *9*(2), 587–606. https://doi.org/10.5194/gmd-9-587-2016

Allen, E. B., Allen, M. F., Helm, D. J., Trappe, J. M., Molina, R., & Rincon, E. (1995). Patterns and regulation of mycorrhizal plant and fungal diversity. *Plant and Soil*, *170*(1), 47–62. https://doi.org/10.1007/BF02183054

Allen, K., Fisher, J. B., Phillips, R. P., Powers, J. S., & Brzostek, E. R. (2020). Modeling the Carbon Cost of Plant Nitrogen and Phosphorus Uptake Across Temperate and Tropical Forests. *Frontiers in Forests and Global Change*, *3*. https://doi.org/10.3389/ffgc.2020.00043

Bailey, R. G. (2014). *Ecoregions: The ecosystem geography of the oceans and continents*. *Ecoregions: The Ecosystem Geography of the Oceans and Continents*. Springer New York. https://doi.org/10.1007/978-1-4939-0524-9

Bartholomé, E., & Belward, A. S. (2005). GLC2000: a new approach to global land cover mapping from Earth observation data. *International Journal of Remote Sensing*. https://doi.org/10.1080/01431160412331291297

Braghiere, R. K., Quaife, T., Black, E., He, L., & Chen, J. M. (2019). Underestimation of Global Photosynthesis in Earth System Models Due to Representation of Vegetation Structure. *Global Biogeochemical Cycles*, *33*(11), 1358–1369. https://doi.org/10.1029/2018GB006135

Brzostek, E. R., Fisher, J. B., & Phillips, R. P. (2014). Modeling the carbon cost of plant nitrogen acquisition: Mycorrhizal trade-offs and multipath resistance uptake improve predictions of retranslocation. *Journal of Geophysical Research: Biogeosciences*, *119*(8), 1684–1697. https://doi.org/10.1002/2014JG002660

Cheng, S. J., Hess, P. G., Wieder, W. R., Thomas, R. Q., Nadelhoffer, K. J., Vira, J., et al. (2019). Decadal fates and impacts of nitrogen additions on temperate forest carbon storage: a data–model comparison. *Biogeosciences*, *16*(13), 2771–2793. https://doi.org/10.5194/bg-16-2771-2019

ESA. (2017). CCI Land cover map 2015.

Fisher, J. B., Sitch, S., Malhi, Y., Fisher, R. A., Huntingford, C., & Tan, S.-Y. (2010). Carbon cost of plant nitrogen acquisition: A mechanistic, globally applicable model of plant nitrogen uptake, retranslocation, and fixation. *Global Biogeochemical Cycles*, *24*(1), n/a-n/a. https://doi.org/10.1029/2009GB003621

Fisher, R. A., Wieder, W. R., Sanderson, B. M., Koven, C. D., Oleson, K. W., Xu, C., et al. (2019). Parametric Controls on Vegetation Responses to Biogeochemical Forcing in the CLM5. *Journal of Advances in Modeling Earth Systems*, *11*(9), 2879–2895. https://doi.org/10.1029/2019MS001609

Ghimire, B., Riley, W. J., Koven, C. D., Mu, M., & Randerson, J. T. (2016). Representing leaf and root physiological traits in CLM improves global carbon and nitrogen cycling predictions. *Journal of Advances in Modeling Earth Systems*. https://doi.org/10.1002/2015MS000538

Kennedy, D., Swenson, S., Oleson, K. W., Lawrence, D. M., Fisher, R., Lola da Costa, A. C., & Gentine, P. (2019). Implementing Plant Hydraulics in the Community Land Model, Version 5. *Journal of Advances in Modeling Earth Systems*, *11*(2), 485–513. https://doi.org/10.1029/2018MS001500

Kim, H. (2017). Global Soil Wetness Project Phase 3 Atmospheric Boundary Conditions (Experiment 1). Data Integration and Analysis System (DIAS). https://doi.org/https://doi.org/10.20783/DIAS.501

Kriegler, E., Bauer, N., Popp, A., Humpenöder, F., Leimbach, M., Strefler, J., et al. (2017). Fossil-fueled development (SSP5): An energy and resource intensive scenario for the 21st century. *Global Environmental Change*, *42*, 297–315. https://doi.org/10.1016/j.gloenvcha.2016.05.015

Lawrence, D. M., Hurtt, G. C., Arneth, A., Brovkin, V., Calvin, K. V., Jones, A. D., et al. (2016). The Land Use Model Intercomparison Project (LUMIP) contribution to CMIP6: rationale and experimental design. *Geoscientific Model Development*, *9*(9), 2973–2998. https://doi.org/10.5194/gmd-9-2973-2016

Lawrence, D. M., Fisher, R. A., Koven, C. D., Oleson, K. W., Swenson, S. C., Bonan, G., et al. (2019). The Community Land Model Version 5: Description of New Features, Benchmarking, and Impact of Forcing Uncertainty. *Journal of Advances in Modeling Earth Systems*, *11*(12), 4245–4287. https://doi.org/10.1029/2018MS001583

NCAR. (2019). CLM5 Documentation Release, 337.

O'Neill, B. C., Tebaldi, C., Van Vuuren, D. P., Eyring, V., Friedlingstein, P., Hurtt, G., et al.

(2016). The Scenario Model Intercomparison Project (ScenarioMIP) for CMIP6. *Geoscientific Model Development*, *9*(9), 3461–3482. https://doi.org/10.5194/gmd-9-3461-2016

Öpik, M., Vanatoa, A., Vanatoa, E., Moora, M., Davison, J., Kalwij, J. M., et al. (2010). The online database MaarjAM reveals global and ecosystemic distribution patterns in arbuscular mycorrhizal fungi (Glomeromycota). *New Phytologist*, *188*(1), 223–241. https://doi.org/10.1111/j.1469-8137.2010.03334.x

Phillips, R. P., Brzostek, E., & Midgley, M. G. (2013). The mycorrhizal-associated nutrient economy: a new framework for predicting carbon-nutrient couplings in temperate forests. *New Phytologist*, *199*(1), 41–51. https://doi.org/10.1111/nph.12221

Read, D. J. (1991). Mycorrhizas in ecosystems. *Experientia*, *47*(4), 376–391. https://doi.org/10.1007/BF01972080

Reich, P. B., Sendall, K. M., Rice, K., Rich, R. L., Stefanski, A., Hobbie, S. E., & Montgomery, R. A. (2015). Geographic range predicts photosynthetic and growth response to warming in co-occurring tree species. *Nature Climate Change*, *5*(2), 148–152. https://doi.org/10.1038/nclimate2497

Riahi, K., van Vuuren, D. P., Kriegler, E., Edmonds, J., O'Neill, B. C., Fujimori, S., et al. (2017). The Shared Socioeconomic Pathways and their energy, land use, and greenhouse gas emissions implications: An overview. *Global Environmental Change*, *42*, 153–168. https://doi.org/10.1016/j.gloenvcha.2016.05.009

Shi, M., Fisher, J. B., Brzostek, E. R., & Phillips, R. P. (2016). Carbon cost of plant nitrogen acquisition: global carbon cycle impact from an improved plant nitrogen cycle in the Community Land Model. *Global Change Biology*, *22*(3), 1299–1314. https://doi.org/10.1111/gcb.13131

Soudzilovskaia, N. A., van Bodegom, P. M., Terrer, C., Zelfde, M. van't, McCallum, I., Luke McCormack, M., et al. (2019). Global mycorrhizal plant distribution linked to terrestrial carbon stocks. *Nature Communications*, *10*(1), 5077. https://doi.org/10.1038/s41467-019-13019-2

Steidinger, B. S., Crowther, T. W., Liang, J., Van Nuland, M. E., Werner, G. D. A., Reich, P. B., et al. (2019). Climatic controls of decomposition drive the global biogeography of forest-tree symbioses. *Nature*, *569*(7756), 404–408. https://doi.org/10.1038/s41586-019-1128-0

Sulman, B. N., Shevliakova, E., Brzostek, E. R., Kivlin, S. N., Malyshev, S., Menge, D. N. L., & Zhang, X. (2019). Diverse Mycorrhizal Associations Enhance Terrestrial C Storage in a Global Model. *Global Biogeochemical Cycles*, *33*(4), 501–523. https://doi.org/10.1029/2018GB005973

Tedersoo, L., Bahram, M., Põlme, S., Kõljalg, U., Yorou, N. S., Wijesundera, R., et al. (2014). Global diversity and geography of soil fungi. *Science*, *346*(6213), 1256688. https://doi.org/10.1126/science.1256688

Xu, C., Fisher, R., Wullschleger, S. D., Wilson, C. J., Cai, M., & McDowell, N. G. (2012). Toward a mechanistic modeling of nitrogen limitation on vegetation dynamics. *PLoS ONE*, *7*(5), 1–11. https://doi.org/10.1371/journal.pone.0037914